Sources and detection of gravitational waves

Adamantios Stavridis

Department of physics

ARISTOTLE UNIVERSITY OF THESSALONIKI

Contents

I. INTRODUCTION

According to general relativity, compact concentrations of energy (e.g, neutron stars, black holes) should warp spacetime strongly, and whenever such an energy concentration changes shape, it should create a dynamically changing spacetime warpage that propagates out through the Universe at the speed of light. This propagating warpage is called gravitational radiation -a name which arises from general relativistic description of gravity as a consequence of spacetime warpage. Like water waves on the ocean the concept of a gravitational wave requires the idealization of a smooth, unperturbed background on which the waves propagate. Unlike water waves, however, gravitational waves are not motion in a material medium; they are ripples in the fabric of spacetime itself. Once the waves leave their sources (near zone), they exist generally in regions where their wavelengths λ are very small compared to the radius of curvature R of the background spacetime through which they propagate.

Gravitational waves have two linear polarizations, conventionally called + (plus) and $\times$ (cross). Associated with each polarization there is a gravitational-wave field, h_+ and $h_\times$, which oscillates in time and propagates with the speed of light. Each wave field produces tidal forces (stretching and squeezing forces) on any object or detector through which it passes. Relative to the object's center, the forces have the quadrupole patterns shown in Fig. 1.

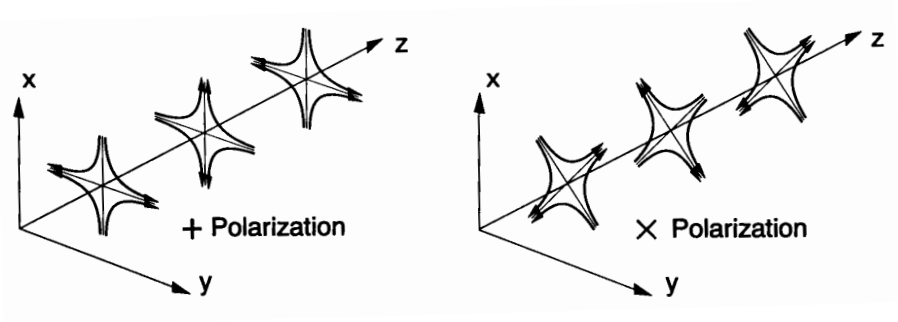

FIG. 1. The lines of force associated with the two polarizations of a gravitational wave.

There are great differences between the gravitational waves and the electromagnetic

waves.

1. Electromagnetic waves are oscillations of the electromagnetic field that propagate through spacetime; gravitational waves are oscillations of the spacetime itself, as I mentioned above.

2. Electromagnetic waves are almost always incoherent superpositions of emission from individual electrons, atoms, and molecules. Gravitational waves are produced by coherent, bulk motions of huge amounts of mass-energy or the energy of vibrating, nonlinear spacetime curvature.

3. Electromagnetic waves are easily absorbed, scattered, and dispersed by matter. Gravitational waves travel nearly unscattered through all amounts of intervening matter.

4. Electromagnetic waves have frequencies that begin at $f \sim 10^7$ Hz and extend upward by roughly 20 orders of magnitude. Gravitational waves frequencies should begin at $f \sim 10^4$ Hz and extend downwards by roughly 20 orders of magnitude.

5. Since the wavelengths of the electromagnetic waves are small compared to their sources (gas clouds, stellar atmospheres, accretion discs), from the waves we can make pictures of the sources. The wavelengths of gravitational waves are comparable to or larger than their sources, so we cannot make pictures of their sources. Instead, the gravitational waves are like sound; they carry, in two independent waveforms, a stereophonic, description of their sources.

These enormous differences make it likely that most (but not all) gravitational waves sources that our instruments detect will not be seen electromagnetically, and vice versa. For example, typical electromagnetic wave sources are stellar atmospheres, accretion disks, and clouds of interstellar gas —none of which emit significant gravitational waves— while typical gravitational waves sources are the cores of supernovae (which are hidden from electromagnetic view by dense layers of surrounding stellar gas), and colliding black holes (which emit no electromagnetic radiation at all).

We are sure about the existence of gravitational waves since we know that the orbital frequency of the binary pulsar PSR1913+16 is increasing with time due to the emission of gravitational radiation. But our desire is to "see" gravitational waves directly and not indirectly by their consequences. There are a number of efforts, worldwide, to detect gravitational waves. These efforts are driven in part by the desire to "see gravitational waves alive," as I mentioned earlier, but more importantly by the goal of using the waves as a probe of the Universe and of the nature of gravity. They should be a powerful probe, since they carry very detailed information about gravity and their sources.

This paper is organized as follows:

In Sec. II, I will refer to possible sources of gravitational radiation, that is supernova explosions, coalescing binaries, pulsars, big bang etc. I will make a detailed reference to the coalescing binaries and pulsars because their study is easier and more understandable.

In Sec. III, I will mention the two kind of detectors that are developed for catching gravitational waves and the methods we use to search the signals in the noisy output of the detectors.

Finally, in Sec. IV, I will analyse the " inverse problem ", namely the way to extract from a gravitational wave signal the parameters of its source.

II. SOURCES OF GRAVITATIONAL RADIATION

A. Coalescing compact binaries

The best understood of all gravitational wave sources are coalescing compact binaries composed of neutron stars (NS) or black holes (BH). The famous Hulse-Taylor binary pulsar is an example of a NS/NS binary whose waves could be measured by LIGO/VIRGO, if we were to wait long enough. At present the PSR1913+16 has an orbital frequency of about 1/(8h) and emits its waves at twice this frequency, roughly 10^{-4} Hz. This is far outside the LIGO/VIRGO band. However, as a result of their lose of orbital energy to gravitational

waves, the PSR1913+16 neutron stars are gradually spiraling inward. If we wait 10^8 years, this inspiral will bring the waves into the LIGO/VIRGO band ($\sim$ 10 Hz to 10^3 Hz). As the two stars continue their inspiral the wave's frequency will then increase over a time of about 15 min from 10 Hz to 10^3 Hz, at which point the two stars will collide and coalesce. It is these last 15 minutes of the inspiral, with $\sim$ 16.000 cycles of waveform oscillation, and the final coalescence that the LIGO/VIRGO seeks to monitor.

The important question that arises is how many of these systems exist in our Galaxy and generally in the close Universe. According to estimates by Narayan, Piran, Shemi and Phinney based on statistics of binary pulsar searches and discoveries, in our Galaxy there is one every 100.000 years. Extrapolating out through the Universe we find that we have to look out to a distance of 200 Mpc (give or take a factor $\sim$ 2) to have some hope to detect such waves in a reasonable time.

The observationally inferred coalescence rate is roughly 100 times smaller than the birth rate of the NS/NS binaries' progenitors; that are massive, compact, main-sequence binaries. Therefore, either 99% of progenitors fail to make it to the NS/NS state (e.g, because of binary disruption during a supernova), or else they do make it, but they wind up as a class of NS/NS binaries that has not yet been discovered in any of the pulsar searches. If the latter is the case, then the coalescence rate in our galaxy will be one per 1000 years and so the LIGO/VIRGO will have to look out to about 40 Mpc rather than 200 Mpc to see a few coalescing binaries per year.

1. Inspiral wave forms and the information they carry

Neutron stars and black holes have such intense gravity that is exceedingly difficult to deform them. Correspondingly, as they spiral inward in a compact binary, they do not gravitationally deform each other significantly until several orbits before their final coalescence. This means that the inspiral wave forms are determined to high accuracy by only a few parameters: the masses and spin angular momentum of the bodies and their

initial orbital parameters (the parameters when the wave enters the detector).

Although tidal deformations are negligible during inspiral, relativistic effects can be very important. If we neglect those effects and approximate gravity as Newtonian we will get the following for a binary system: (We assume that the two bodies move on circular orbits around their center of mass). The kinetic energy of each body, and the total kinetic energy of the system are, respectively,

$$T_1 = \frac{G\mu m_2}{2R}, \;\; T_2 = \frac{G\mu m_1}{2R}, \;\; T_{\rm tot} = \frac{G m_1 m_2}{2R}, \tag{1}$$

where m_1, m_2 are the masses of the two stars, μ is the reduced mass of the system $\mu = m_1 m_2 / m_1 + m_2$ and R is the distance between the two stars. The potential energy of the system is :

$$V = -\frac{G m_1 m_2}{R}. \tag{2}$$

So the total energy of the system is

$$E_{\rm tot} = -\frac{G m_1 m_2}{2R}. \tag{3}$$

But we know from general relativity that the energy loss rate is given by

$$\frac{dE}{dt} = -\frac{1}{5}\frac{G}{c^5}\langle \dddot{I}_{ij} \dddot{I}_{ij} \rangle = \frac{32}{5}\frac{G^4}{c^5}\frac{M^3 \mu^2}{R^5}. \tag{4}$$

By combining the above equation with Eq. (3) and by solving with respect to R we get the expression below for $R(t)$:

$$R(t) = \left(\frac{256 G^3 m_1 m_2 M}{5c^5} \right)^{1/4} (t_c - t)^{1/4}, \tag{5}$$

where c is the speed of light, M is the total mass and t_c is the so called coalescence time, which is the time the two stars will coalesce. Taking under consideration the relation between ω and R we get the expression for $\omega(t)$, which is

$$\omega_{\rm bin}(t) = a \mathcal{M}^{-5/8} (t_c - t)^{-3/8}, \tag{6}$$

where $a = G^{-5/8} \left(\frac{256}{5c^5} \right)^{-3/8}$ and $\mathcal{M}$ is the so called chirp mass defined as $\mathcal{M} \equiv \left(\frac{M_1^3 M_2^3}{M_1 + M_2} \right)^{1/5}$.

From the above equation we are able to find the phase of the wave, which is $\phi = \int \omega(t) dt$. After integration we obtain,

$$\phi_{\rm bin}(t) = -\frac{8}{5} a \mathcal{M}^{-5/8} (t_c - t)^{5/8} + \phi_c, \tag{7}$$

where ϕ_c, is an initial phase. The final step is to get the strain of the gravitational wave $h(t)$, which is, according to the Newtonian quadrupole moment approximation,

$$h(t) = \frac{Q(\theta, \phi, \psi, i) \mu M}{DR(t)} cos \left(\int \omega_{\rm wav} dt \right), \tag{8}$$

where, $Q(\theta, \phi, \psi, i)$ is a factor depending on the geometry of the detector-binary system and D is the distance to the source. If we use equations (5) and (7) then we obtain for the strain of the gravitational wave (neglecting the geometry parameter Q):

$$h(t) = \frac{2}{D} \left(\frac{5c^5}{256 G^3} \right)^{1/4} \mathcal{M}^{5/4} (t_c - t)^{-1/4} \cos \left(-\frac{16}{5} a \mathcal{M}^{-5/8} (t_c - t)^{5/8} + \phi_c \right). \tag{9}$$

Here notice that the frequency of the gravitational waves emitted is double the frequency of the binary, $\omega_{\rm wav} = 2\omega_{\rm bin}$ and therefore $\phi_{\rm wav} = 2\phi_{\rm bin}$, this is because the quadropole moment repeats when the masses move through one half of their orbit. The shape of the waveform is shown in Fig. 2.

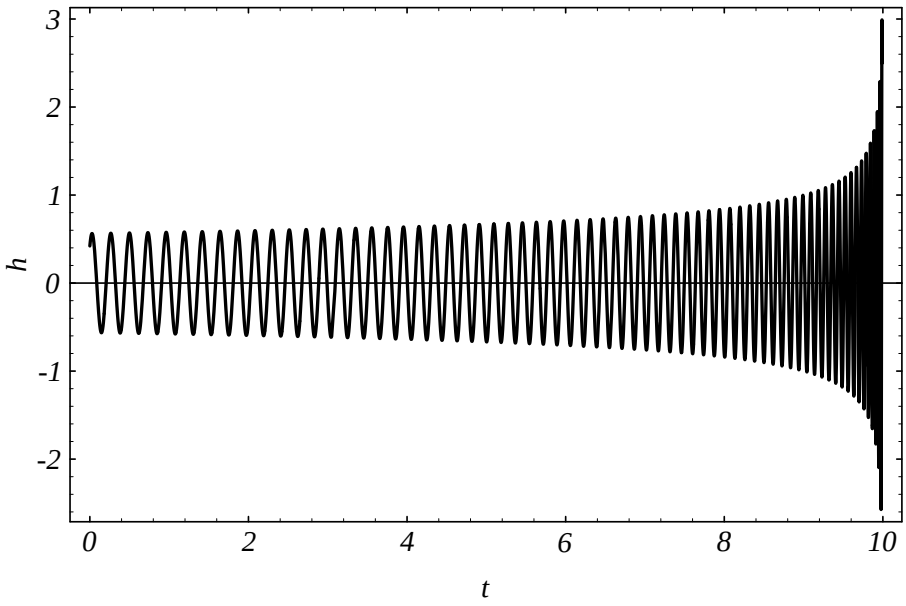

FIG. 2. The waveform of Eq. (9). The amplitude and the frequency of the wave are increasing with time.

As one can see from the diagram, the amplitude and the frequency of the signal are increasing as the binary bodies spiral closer and closer together. Because of that, the signal is referred to as 'chirp' (a term that comes from the radar technique). The ratio of the amplitudes of the two polarizations is determined by the inclination i of the orbital plane to the line of our sight from the relation

$$\frac{\mathrm{Amp}(\mathrm{h_x})}{\mathrm{Amp}(\mathrm{h_+})} = \frac{2\cos i}{1+\cos^2 i}. \tag{10}$$

The shapes of the individual waves, are determined by the orbital eccentricity. In our case of a circular orbit the rate at which the frequency sweeps, df/dt, is determined solely, in the Newtonian approximation, by the binary's chirp mass. The amplitude of the two waveforms are determined by the chirp mass, the distance to the source, and the orbital

inclination. Thus, by measuring the two amplitudes (in the Newtonian approximation), the frequency sweep, and the harmonic content of the inspiral waves, we can determine the source's distance, chirp mass, inclination and eccentricity (if there is any).

2. Coalescence waveforms and their information

The waves from the binary's final coalescence can bring us new types of information. In the case of a BH/BH binary, the coalescence will excite large-amplitude, highly nonlinear vibrations of spacetime curvature near the coalescing black-hole horizons —a phenomenon of which we have little understanding today. Especially fascinating will be the case of two spinning black holes whose spins are not alligned with each other or with the orbital angular momentum. The dynamical evolution of such a complex configuration of coalescing spacetime warpage (as revealed by its emitted waves) might bring us surprising new insights into relativistic gravity. Moreover if the sum of the BH masses is fairly large $\simeq$ 40 to 200$M_\odot$, then the waves should have frequencies of about 200 to 40 Hz where the LIGO/VIRGO broad-band interferometers have their best sensitivity and can best extract the informations the wave carry. The challenge of computing the waves from such a coalescence, via supercomputer simulations, appear to be almost as difficult as detecting them, especially if the holes are spinning and their spins and their orbital angular momentum are not alligned, as I said above. High priority is given to the development of such simulations, so that, when the LIGO/VIRGO detectors begin to monitor BH/BH coalescences, comparison of theory and experiment can be used to unravel the details of the nonlinear vibrations of spacetime curvature.

The final coalescence of NS/NS binaries should produce waves that are sensitive to the equation of state of nuclear matter so that coalescences have the potential to teach us about the nuclear equation of state. Unfortunately, the final NS/NS coalescence will emit its gravitational radiation in the kHz frequency band (800 Hz $< f <$ 2500 Hz) where photon shot noise will prevent them from being studied by the LIGO/VIRGO interferometers, but

only by resonant bars and spherical detectors. A number of research groups [19] are engaged in numerical astrophysics simulations of NS/NS coalescence, with the goal not only to predict the emitted gravitational waveforms and their dependence on equation of state, but also to learn whether such coalescences power the γ-ray bursts that have been a major astronomical puzzle since their discover in early 70s. NS/NS coalescence is currently a popular explanation for the γ-ray bursts because (1) the bursts are isotropically distributed on the sky, (2) they have a distribution of number versus intensity that suggests they might lie at near-cosmological distances, and (3) their event rate is roughly the same as that predicted for NS/NS coalescence. If LIGO/VIRGO were now in operation and observing NS/NS inspirals, they could report definitely whether or not the γ bursts are produced by NS/NS binaries; and if the answer were yes, then the combination of the γ-bursts data and gravitational-wave data could bring valuable information that neither of them could bring by itself. For example, it would reveal when, to within a few msec, the γ-burst is emitted relative to the moment the NS's first begin to touch; and by comparing the γ and the gravitational-wave times of arrival, we might test whether gravitational waves propagate with the speed of light to a fractional precision of $\simeq 0.01\text{sec}/3 \times 10^9\text{lyr} = 10^{-19}$.

A NS spiraling into a BH of mass $M \geq 10M_\odot$ should be swallowed more or less as a whole. However, if the BH is less massive than roughly $10M_\odot$, and especially if it is rapidly rotating, then the NS will tidally disrupt before being swallowed. Little is known about the disruption and corresponding waveforms. To model them with any reliability will likely require full numerical relativity, since the circumferences of the BH and the NS will be comparable and their physical separation at the moment of disruption will be of the order of their separation. As with the NS/NS coalescence their waves should carry information about the equation of state information and will come out in the kHz band where their detection will require interferometric gravitational detectors working in dual recycling mode.

B. Spinning neutron stars—Pulsars

An axisymmetric object rotating rigidly about its symmetry axis has no time-varying quadropole moment, and hence does not radiate gravitational radiation.

If the principal moments of inertia of an object are I_1, I_2, I_3, then radiation will be produced if it rotates about the principal axis $\mathbf{e_3}$ and is nonaxisymmetric ($I_1 \neq I_2$). Alternatively, it can radiate if it is axisymmetric ($I_1 = I_2$), but the rotation axis is not a symmetry axis e_3. I shall consider the first case first, whose physical application could be a pulsar whose rigid crust can support a "mountain". A set of coordinates x_i', rotating with the object (body coordinates) is related to an inertial coordinate system x_i with common origin at the center of the mass by the rotation matrix:

$$x' = Rx \tag{11}$$

where,

$$R_{ij} = \begin{pmatrix} \cos\phi & \sin\phi & 0 \\ -\sin\phi & \cos\phi & 0 \\ 0 & 0 & 1 \end{pmatrix} \tag{12}$$

and $\phi = \Omega t$; $\Omega = constant$ (no applied torques). The inertia tensor in the inertial coordinates has components given by

$$I = R^T I' R, \tag{13}$$

where I' is a diagonal matrix with diagonal elements I_1, I_2 and I_3. I will use 1,2,3 to denote components in the body frame and x,y,z for the inertial frame. The components of the inertia tensor in the inertial frame are

$$I_{xx} = I_1 \cos^2\phi + I_2 \sin^2\phi = \frac{1}{2}(I_1 - I_2)\sin 2\phi + \text{const}, \tag{14a}$$

$$I_{xy} = I_{yx} = \frac{1}{2}(I_1 - I_2)\sin 2\phi, \tag{14b}$$

$$I_{yy} = \frac{1}{2}(I_2 - I_1)\cos 2\phi + \text{const}, \tag{14c}$$

$$I_{zz} = \text{const}, \tag{14d}$$

$$I_{xz} = I_{yz} = I_{zx} = I_{zy} = 0, \tag{14e}$$

since $TrI' = TrI = I_1 + I_2 + I_3 = \text{constant}$, we can use I_{ij} instead of I_{ij} in the energy loss formula and thus we get

$$\begin{aligned}\frac{dE}{dt} &= -\frac{1}{5}\frac{G}{c^5}\langle \dddot{I}^2_{xx} + \dddot{I}^2_{yy} + \dddot{I}^2_{zz}\rangle \\ &= -\frac{1}{20}\frac{G}{c^5}(2\Omega)^6(I_1 - I_2)^2\langle \cos^2 2\phi + 2\sin^2 2\phi + \cos^2 2\phi\rangle \\ &= -\frac{32}{5}\frac{G}{c^5}(I_1 - I_2)^2\Omega^6. \end{aligned} \tag{15}$$

If the object can be approximated by a homogeneous ellipsoid with semi axes a,b,c then

$$I_1 = \frac{1}{5}M(b^2 + c^2), \tag{16a}$$

$$I_2 = \frac{1}{5}M(a^2 + c^2), \tag{16b}$$

$$I_3 = \frac{1}{5}M(a^2 + b^2), \tag{16c}$$

For a small asymmetry(i.e, $a \simeq b$), we may write

$$\frac{dE}{dt} \simeq -\frac{32}{5}\frac{G}{c^5}I_3^2\epsilon^2\Omega^6 \tag{17}$$

where the ellipticity ϵ is defined by

$$\epsilon = \frac{(a-b)}{(a+b)/2}. \tag{18}$$

Now turn to the case of rigid rotation about a nonprincipal axis, but assume $I_1 = I_2$, for simplicity. Choose the fixed direction of the angular momentum vector $\mathbf{J}$ to be along $\mathbf{e_z}$

in the inertial frame. The transformation to the body coordinates is given in terms of the Euler angles by

$$R_{ij} = \begin{pmatrix} \cos\psi\cos\phi - \cos\theta\sin\phi\sin\psi & \cos\psi\sin\phi + \cos\theta\cos\phi\sin\psi & \sin\theta\sin\psi \\ -\sin\psi\cos\phi - \cos\theta\sin\phi\cos\psi & -\sin\psi\sin\phi + \cos\theta\cos\phi\cos\psi & \sin\theta\cos\psi \\ \sin\theta\sin\phi & -\sin\theta\cos\phi & \cos\theta \end{pmatrix} \tag{19}$$

In free precession, the symmetry axis $\mathbf{e_3}$ and the angular velocity vector rotate about $\mathbf{e_z}$ with constant angular velocity $\dot{\phi} = J/I_1$, $\mathbf{e_3}$ maintaining a constant angle θ with respect to $\mathbf{e_z}$. In addition the angular velocity vector precesses about $\mathbf{e_3}$ with angular velocity $\dot{\psi} = (I_1 - I_3)\dot{\phi}\cos\theta/I_3 = \text{constant}$, as seen in the body frame. Equations (13) and (19) give

$$\begin{aligned} I_{xx} &= I_1(\cos^2\phi + \cos^2\theta\sin^2\phi) + I_3\sin^2\theta\sin^2\phi \\ &= \frac{1}{2}(I_1 - I_3)\sin^2\theta\cos^2 2\phi + \text{constant}, \end{aligned} \tag{20a}$$

$$I_{xy} = I_{yx} = \frac{1}{2}(I_1 - I_3)\sin^2\theta\sin 2\phi, \tag{20b}$$

$$I_{xz} = I_{zx} = -(I_1 - I_3)\sin\theta\cos\theta\sin\phi, \tag{20c}$$

$$I_{yy} = -\frac{1}{2}(I_1 - I_3)\sin^2\theta\cos 2\phi + \text{constant}, \tag{20d}$$

$$I_{yz} = I_{zy} = (I_1 - I_3)\sin\theta\cos\theta\cos\phi, \tag{20e}$$

$$I_{zz} = I_3 + (I_1 - I_2)\sin^2\theta = \text{constant}. \tag{20f}$$

Writting $\phi = \Omega t$, $\Omega = \dot{\phi} = \text{constant}$, we find

$$\begin{aligned} \frac{dE}{dt} &= -\frac{1}{5}\frac{G}{c^5}\langle \dddot{I}_{xx}^2 + \dddot{I}_{yy}^2 + 2\dddot{I}_{xy}^2 + 2\dddot{I}_{xz}^2 + 2\dddot{I}_{yz}^2 \rangle \\ &= -\frac{1}{5}\frac{G}{c^5}(I_1 - I_3)^2\langle \frac{1}{4}\sin^4\theta(2\Omega)^6(2\cos^2 2\phi + 2\sin^2 2\phi) + 2\Omega^6\sin^2\theta\cos^2\theta(\cos^2\phi + \sin^2\phi)\rangle \\ &= -\frac{2}{5}\frac{G}{c^5}(I_1 - I_3)^2\Omega^6\sin^2\theta(16\sin^2\theta + \cos^2\theta). \end{aligned} \tag{21}$$

For a small "wobble angle" θ, we get

$$\frac{dE}{dt} \simeq -\frac{2}{5}\frac{G}{c^5}(I_1 - I_3)^2\Omega^6\theta^2. \tag{22}$$

Note that for rotation about a principal axis (Eqs. (15) and (17)) the frequency of the radiation is 2Ω. In the case of Eqs. (21) and (22), however, the dominant radiation is at frequency Ω, since the $\cos^2\theta$ term comes from I_{xz} and I_{yz}. In the general case of combined "mountain" and "wobble" radiation, dE/dt is given by the sum of Eqs. (15) and (21), provided the "mountain" and the "wobble" are small.

As a neutron star settles down into it's final state, its crust begins to solidify (crystalize). The solid crust will assume nearly the oblate axisymmetric shape that centrifugal forces are trying to maintain, with poloidal ellipticity $\epsilon_p \sim \omega^2$. However, the principal axis of the star's moment of inertia tensor may deviate from its spin axis by some small "wobble angle" θ_w, and the star may deviate slightly from axisymmetry about its principal axis; i.e., it may have a slight ellipticity $\epsilon_e \ll \epsilon_p$ in its equatorial plane.

As this slightly imperfect crust spins, it will radiate gravitational waves with frequency twice the frequency of the rotation, $f = 2f_r$ with $h \sim \epsilon_e$, and the wobble angle will couple to ϵ_p producing waves at $f = f_{\rm rot} + f_{\rm prec}$ (the precessional sideband of the rotation frequency) with amplitude $h \sim \theta_w \times \epsilon_p$. For typical neutron-star masses and moments of inertia, the wave amplitudes are

$$h \sim 6 \times 10^{-25} \left(\frac{f_{\rm rot}}{500{\rm Hz}}\right)^2 \left(\frac{1{\rm kpc}}{r}\right) \left(\frac{\epsilon_e \text{ or } \theta_w\epsilon_p}{10^{-6}}\right) \ . \tag{23}$$

The neutron star gradually spins down, due in parts to gravitational-wave emission but perhaps mainly due to electromagnetic torques associated with its spinning magnetic field and pulsar emission. The spin-down reduces the strength of centrifugal forces, and thereby causes the star's poloidal ellipticity ϵ_p to decrease with resulting breakage and resolidification of its crust's crystal structure. In each starquake, θ_w, ϵ_e and ϵ_p will all change suddenly, thereby changing the amplitudes and frequencies of the star's two gravitational " spectral lines " $f = 2f_{\rm rot}$ and $f = f_{\rm rot} + f_{\rm prec}$. After each quake, there should be a healing period

in which the star's fluid core and solid crust, now rotating at different speeds, gradually regain synchronism. By monitoring the amplitudes, frequencies, and phases of the two gravitational-wave spectral lines, and by comparing them with timing of the electromagnetic pulsar emission, one might learn much about the physics of the neutron star interior.

But how large the quantities ϵ_e and $\theta_w \times \epsilon_p$ will be? Rough estimates of the crystal shear moduli and breaking strengths suggest an upper limit in the range $\epsilon_{\max} \sim 10^{-4}$ to 10^{-6}, and it might be that typical values are far below this. We are extremely ignorant, and correspondingly there is much to be learned from searches for gravitational waves from spinning neutron stars.

C. Supernovae

Traditionally supernovae are classified into two classes: type I supernovae (SNI) and type II supernovae (SNII). Type II supernovae represent the core collapse of a massive star and the shock-driven rebound expansion of an optically luminous shell. In a few instances it is certain that the collapsed core is a neutron star. Type I supernovae are different. The traditional view is that a type I supernovae is the nuclear detonation of a white dwarf, after it has accreted matter from a companion. There appear to be many reasons why this may not be correct however. The white dwarf has the choice of collapsing or detonating and the choice is determined by detailed properties of degenerate matter. The best guess today is that it is likely that at least a fraction of accreting white dwarfs will collapse, but only to a neutron star, since white dwarf mass is insufficient to allow collapse to a black hole.

Supernovae 1987A discovered on February 23, 1987, represented a historic landmark in astronomy. The supernovae occured in a nearby irregular dwarf galaxy, the Large Magellanic Cloud, at a distance of about 50 Kpc. In this instance neutrinos from the inverse β-decay associated with the collapse were observed by several huge detectors originally designed to test for the radioactive decay of protons. This is the first instance of direct observation of core collapse.

The strengths of gravitational waves from a supernovae depend crucially on the degree of non-sphericity in the stellar collapse that triggers it, and somewhat on the speed of the collapse. Perfectly spherical collapse will produce no waves; highly non-spherical collapse will produce strong waves. The main source of non-sphericity during collapse is angular momentum. Little is known about the degree of non-sphericity in type II but current prejudice suggests that the typical type II might be quite spherical and thus poorly radiating. About type I on the contrary, if are due to explosion of an accreting white dwarf, the explosion is accompanied by collapse of the stellar core to a neutron star, then the white dwarf might be rapidly rotating due to the accretion, and the centrifugal forces might then cause it to collapse very non-spherically and radiate strongly.

Our knowledge about the strengths of the waves and the waveforms from supernovae is poor. The figures below show some typical calculated waveforms, all showing the general character of burst source; extremely brief pulses with duration of only a few cycles. The left curve shows several epochs labeled FF in which $h_+(t)$ varies approximately as $|t - t_0|^{-2/3}$, corresponding to free-fall motion; and these free-fall epochs are separated by three brief periods with sharply reversed peaks (labeled P in the diagram) corresponding to a sharp acceleration in the direction opposite to the free fall. The natural and correct interpretation of the diagram is that these waves are produced from collapse to a neutron star in which the stellar core bounced sharply three times. The fact that the three sharp peeks are all in the direction (up, not down) indicates that the sharp bounces are along the same axis. Surely the other axis that projects on our sky should have bounced as well, or at least stop its collapse; so there should be at least one sharp peak in the down direction. And indeed there is; it is superposed on the central up peak (region labeled E in the diagram). The interpretation of that is that the star was centrifugally flattened by rotation; its pole collapsed fast and bounced three times (up peaks P) while its equator collapsed more slowly and bounced once (down peak E). The entire event lasts only 50 ms. The right curve shows the waveform where the collapse has excited quadropole oscillations of the neutron star. Near sinusoidal oscillations are excited at 1.4 kHz, and rapidly damped out.

Now turn to the formation of black holes due to a star's collapse. It is very likely that black holes exist in our universe with masses throughout a range $2M_\odot \leq M \leq 10^{10} M_\odot$. The holes of lowest mass can only form by direct collapse of a star. Those of higher mass, however, can form by many ways (direct collapse; gradual growth from a small hole by accretion; collision and coalescence of small holes; etc).

In one respect collapse to a black hole is better understood than collapse to a neutron star; the final object is much simpler, and correspondingly the waves from its vibrations, if they are triggered by the collapse, are far better understood. Detailed calculations suggest, in fact, that black hole vibrations are rather easy to trigger and that when they are triggered, the most slowly damped one or two quadropole modes will dominate. Thus, while the details of the initial burst of waves may depend on unknown details of the collapse, the late-time behavior will have a well established damped oscillatory form, from which one can read off the mass of the hole with excellent accuracy and it's angular momentum with modest accuracy.

If collapse to a black hole radiates with an efficiency $\Delta E/Mc^2 = \epsilon$ and the hole is at a distance r_o, and has mass M, then the characteristic frequency and amplitude of its waves will be

$$f_c \simeq \frac{1}{5\pi M} = (1.3 \times 10^4 \mathrm{Hz}) \left(\frac{\mathrm{M}}{\mathrm{M}_\odot}\right), \tag{24a}$$

$$h_c \simeq 1.0 \times 10^{-20} \left(\frac{\epsilon}{0.01}\right)^{1/2} \left(\frac{10^3 \text{ Hz}}{\mathrm{f_c}}\right) \left(\frac{\mathrm{Mpc}}{\mathrm{r_o}}\right). \tag{24b}$$

If the collapse is axisymmetric, then the efficiency ϵ probably doesn't exceed the value of 7×10^{-4}. However, in the non-axisymmetric case the efficiency might be at the range 0.01-0.1.

III. DETECTION OF GRAVITATIONAL WAVES

A. GENERAL REMARKS

The frequency band of gravitational waves can be divided into four regions:

1. The high-frequency band (HF: $f \sim 10^4$ to 1 Hz).

   In this frequency band lies the stellar collapse to a neutron star or a black hole in our Galaxy and distant galaxies; the rotation and vibrations of neutron stars (pulsars) in our Galaxy; the coalescence of neutron star and stellar-mass black hole binaries in distant galaxies.

2. The low-frequency band (LF: $f \sim 1$ to 10^{-4} Hz).

   The low-frequency band should be populated by waves from short-period binary stars in our Galaxy; from white dwarfs, neutron stars and small black holes spiralling into massive black holes ($M \sim 3 \times 10^5$ to 3×10^7) in distant galaxies; and from the inpiral and coalescence of supermassive black-hole binaries (M $\simeq$ 100 to $10^8 M_\odot$).

3. The very-low frequency band (VLF: $f \sim 10^{-7}$ to 10^{-4} Hz).

   The only compact bodies that can radiate in the very-low frequency band at $f \leq 10^{-7}$ Hz are those with $M \geq 10^{11} M_\odot$. Conventional astronomical wisdom suggests that compact bodies this massive cannot exist, and therefore the only strong waves in the VLF band and below are stochastic background produced by cosmic strings, phase radiations and the big bang.

4. The extremely-low frequency band (ELF: $f \sim 10^{-15}$ to 10^{-18} Hz).

   Gravitational waves in the ELF band should produce anisotropies in the cosmic microwave background radiation.

B. DETECTORS

1. BAR DETECTORS

The construction of bar detectors for gravitational radiation is based on the issue of resonance that we know from basic physics. Each body has a normal-mode frequency f_0 which depends on the size and the material of which is made. So our task is to construct bodies from material that have normal-mode frequency equal or similar to the frequencies of gravitational waves we wish to detect. In that case when a gravitational wave hits the detector we have resonance and we might be able to monitor the wave.

In order to understand the function of the bar detector, I analyze the case of a simple quadrupole oscillator consisting of two masses connected by a spring, as a detector of gravitational waves. I want to calculate what oscillation amplitude the incident wave can excite and how much energy is absorbed by the wave. As we know the observable driving force on the oscillator is the tidal force. Suppose that a plane wave is incident on the simple quadrupole placed on x-axis with equilibrium positions $x = \pm b$ which vibrates along this axis and the direction of incidence is perpendicular to that and parallel to one of the principal axes of the tidal deformation field. If the displacement of the two masses remains always small ($\mid x - b \mid \ll b$), then the equation of motion of one of the masses, say, the mass on the positive x-axis, is

$$m\ddot{x} = m\frac{k}{2}A_{\rm wav}\omega^2 b e^{i\omega t} - m\gamma\dot{x} - m\omega_0^2(x-b) \tag{25}$$

where, the first term of the right hand of Eq. (25) is the tidal force, the second is the friction force and the third is the harmonic oscillator force; ω_0, is the natural frequency of the free oscillations and γ is the damping rate associated with the frictional forces acting on the oscillator. The steady-state solution of the above equation is

$$x - b = \frac{\frac{1}{2}kA_{\rm wav}\omega^2 b e^{i\omega t}}{-\omega^2 + \omega_0^2 + i\gamma\omega} \tag{26}$$

where $k = \sqrt{16\pi G}$. The steady state response of the oscillator has a sharp maximum at the frequency $\omega = \omega_0$. Hence gravitational waves of this frequency are in resonance with

the natural oscillations of the system. As a measure of the sensitivity of the detector it is often convenient to use a parameter called the cross section. The scattering cross section is defined as the ratio of the power reradiated to the incident flux , that is

$$\sigma_{\rm scatt}(\omega) = \frac{power\ reradiated}{incident\ flux} \tag{27}$$

and is a parameter that measures the efficiency of the oscillator's scattering the radiation in all directions. The incident flux in this case is $A_{\rm wav}\omega^2/2c$ and the power reradiated is

$$-\left(\frac{d\bar{E}}{dt}\right)_{\rm rad} = \frac{16G}{15c^5}(mAb)^2\omega^6 \tag{28}$$

where A, is the amplitude of the oscillation. Taking A from Eq. (26) and substituting it in the above equation and then in Eq. (27) we obtain for the scattering cross section,

$$\sigma_{\rm scatt} = \frac{15\pi c^2}{2}(\gamma_{\rm rad})^2\frac{1}{(\omega^2-\omega_0^2)^2+\gamma^2\omega^2}, \tag{29}$$

where $\gamma_{\rm rad}$ is

$$\gamma_{\rm rad} = \frac{16G}{15c^5}mb^2\omega^4. \tag{30}$$

Note that $\sigma_{\rm scatt}$ is independent of the amplitude of the incident wave; this is what makes the cross section useful as a measure of how much the quadrupole scatters radiation out of the incident wave.

For the purpose of detecting gravitational waves we are more interested in the energy absorbed from the oscillator than in the one scattered. This means that we want to know what power the oscillator delivers to the (mechanical) frictional forces in the oscillator. In a similar way we can define the absorption cross section as

$$\sigma_{\rm abs}(\omega) = \frac{power\ lost\ to\ mechanical\ friction}{incident\ flux}. \tag{31}$$

We can establish a connection between $\sigma_{\rm abs}$ and $\sigma_{\rm scatt}$, if we note that the total damping rate γ is given by two terms,

$$\gamma = -\frac{1}{E}\left(\frac{d\bar{E}}{dt}\right)_{\rm tot} = -\frac{1}{E}\left(\frac{d\bar{E}}{dt}\right)_{\substack{\rm mechanical\\ \rm friction}} - \frac{1}{E}\left(\frac{d\bar{E}}{dt}\right)_{\rm radiation} = \gamma_m + \gamma_{\rm rad} \tag{32}$$

Thus by definition σ_{scat} and σ_{abs} must stand in the ratio $\gamma_m/\gamma_{\rm rad}$, that is,

$$\sigma_{abs} = \frac{\gamma_m}{\gamma_{\rm rad}}\sigma_{scat}. \tag{33}$$

If we assume that $\gamma_m \gg \gamma_{\rm rad}$ then $\gamma_m \simeq \gamma$ and the σ_{abs} is

$$\sigma_{abs} = \frac{15}{2}\pi c^2 \gamma\gamma_{\rm rad}\frac{1}{(\omega^2-\omega_0^2)^2+\gamma^2\omega^2}. \tag{34}$$

The above calculations were made for a quadrupolar oscillator oriented in the most favorable direction in the tidal field of the wave. The line of vibration of the masses was taken both perpendicular to the direction of incidence and parallel to one of the principal axes of the tidal deformation field. For an oscillator whose masses are constrained to vibrate along a line making an angle θ with the direction of incidence (z-axis) and an angle ϕ with one of the principal axes of the tidal field the component of the tidal force along this line is reduced by a factor

$$\sin^2\theta\cos 2\phi$$

as compared with the most favorable case. This factor is easy to understand; the magnitude of the tidal force is proportional to the transverse dimension of the system ($\sim \sin\theta$) ; taking the component of this force along the line of vibration results another factor $\sin\theta$; finally, the factor $\cos 2\phi$ simply represents the angular dependence of the (radial) tidal field strength in the transverse plane. The cross section depends on the square of the component of the tidal force along the line of vibration; hence the reduce factor is $\sin^4\theta\cos^2 2\phi$. Taking the mean value over all angles of the above factor we get

$$\frac{1}{4\pi}\int \sin^4\theta\cos^2 2\phi d\Omega = \frac{4}{15} \tag{35}$$

Consequently if the wave arrives with an arbitary orientation then the mean $\bar{\sigma}_{\rm abs}$ is

$$\bar{\sigma}_{\rm abs} = 2\pi c^2\gamma\gamma_{\rm rad}\ \frac{1}{(\omega^2-\omega_0^2)^2+\gamma^2\omega^2} \tag{36}$$

Although those calculations have been made for the special case of a simple linear quadrupole, the results are also valid for an arbitary mass system vibrating in a mode

of cylindrical symmetry. More precisely, since the amplitude of the time-dependent part of the quadrupole tensor is some symmetric matrix Q'^{kl}, it can be diagonalized by a transformation to principal axes. By cylindrical symmetry we mean that two of the diagonal elements of the diagonalized matrix are equal. If we take the axis in the z-direction, then $Q'^{11} = Q'^{22}$ and since the trace must be zero, $Q'^{33} = -2Q'^{11}$.

For that reason, a bar detector is usually a cylinder (called resonant mass). The resonant mass is typically made from an alloy of aluminum and weights several tones, but some have been made of niobium or single crystal silikon with masses well below a tone. To control thermal noise, the resonant mass is usually cooled cryogenically to liquid-helium temperatures or below.

The cross-section of a bar detector as a function of frequency is given in Fig. 3.

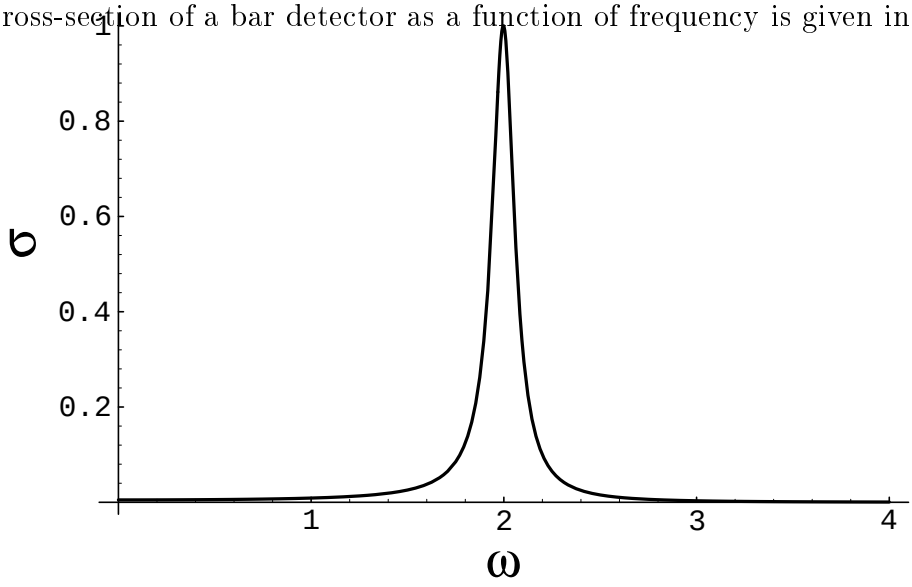

FIG. 3. The cross section of a bar detector as a function of frequency. The maximum is very sharp at the normal-mode frequency. The numbers and units on the diagram are arbitary.

This resonance has a width of only $\Delta f \simeq \gamma/2\pi \simeq 10^{-2} Hz$. Consequently the frequencies of the wave and the normal-mode of the cylinder must agree to one part in $\simeq 10^5$. This is quite unlikely. Probably, the best we can hope is that the radiation contains a spread of frequencies which overlaps the detector resonance; the spread of frequency of the radiation

is likely to be much larger than the width of resonance.

The resonant-mass antenna is instrumented with an electromagnetic transducer and electronics, which monitor the complex amplitude of one or more of the mass's normal modes. When a gravitational wave passes through the mass, its frequency components near each normal-mode frequency f_0 drive that mode, changing its complex amplitude; and the time evolution of the changes is measured within some bandwidth Δf by the transducer and electronics. Current resonant mass antennas are narrow-band devices ($\Delta f/f_0 \ll 1$) but in the era of LIGO/VIRGO, they might achieve bandwidths as large as $\Delta f/f_0 \sim 1/3$

Resonant mass antennas for gravitational radiation were pioneered by Joseph Weber about 35 years ago and have been pushed to even higher sensitivities later. At present there is a network of such antennas, cooled to 3K, and operating with an rms noise level for broad-band gravity-wave bursts of $h_{\rm rms} \simeq 6 \times 10^{-19}$. The network includes an aluminum cylinder called EXPLORER at the University of Rome, Italy; an aluminum cylinder at Louisiana State University, USA; and a niobium cylinder at University of Perth, Australia. This network has been in operation, searching for waves, for several years.

The next generation of resonant-mass antennas is now under construction at the University of Rome and at the University of Legarno, Italy. There are several-ton aluminum bars cooled to 0.05K; their rms sensitivity for wave bursts are $\sim 10^{-20}$.

A subsequent generation, which hopefully will operate in the LIGO/VIRGO era, is being discussed and planned. These are 1 to 100 tone spheres cooled at $\sim$ 0.01-0.05K, with sensitivity goals of $\sim 10^{-22}$. Such antennas might be built by an American collaboration, a Brazilian collaboration, an Italian collaboration called "Omega" , and a Dutch collaboration called "Grail". Their spherical or nearly spherical shapes make them omnidirectional and should give them several times higher sensitivities that can be achieved by cylinders at the same frequency. The name of this program is TIGA (Truncated Icosahedral Gravitational-wave Antenna).

The present consept of the TIGA project is to built a "xylaphone" of four aluminium alloy spheres with diameters ranging from 2 to 3 meters. The largest sphere will then weigh

about 40tons and have the lowest quadropole frequency of about 900 Hz. A three-mode antenna transducer system will allow a fractional bandwidth of about 900 Hz. If both foundamental and second harmonic quadropole modes are instrumented, a frequency range of 800 to 2700 Hz will be covered.

The attractiveness of such antennas in the LIGO/VIRGO era lies in their ability to operate with impressive sensitivity in the uppermost reaches of the high-frequency band, $\sim 10^3$ to 10^4 Hz, where photon shot noise debilitates the performance of interferometric detectors. The figure below shows the projected rms noise curves of TIGA detectors, each instrumented to operate at the "standard quantum limit" for such a detector (a nontrivial experimental task). For comparison is shown the rms noise of the first LIGO interferometer, which of course is not optimized for the kHz band.

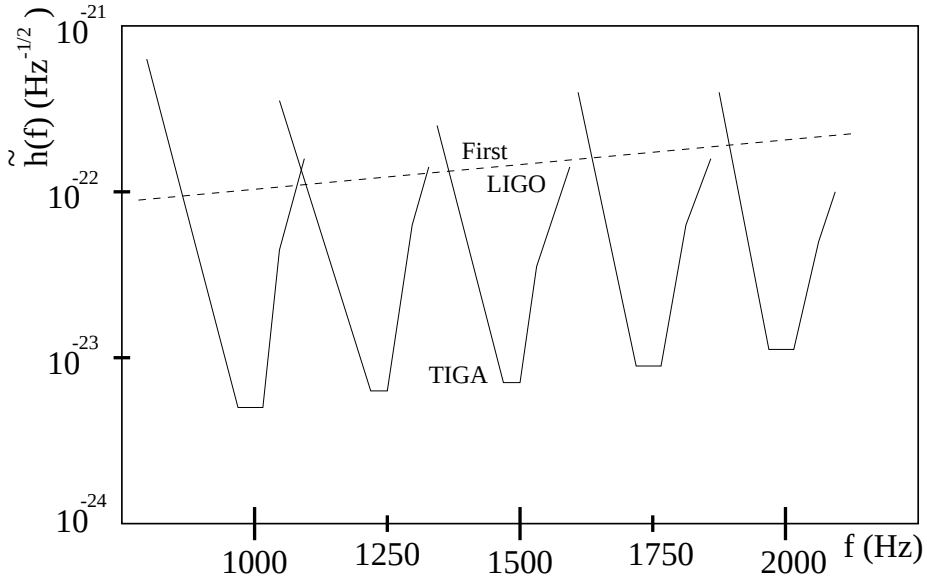

FIG. 4. The rms noise curves $\tilde{h}$ (f) for a 'xylaphone' of TIGA gravitational-wave detectors for signals of random polarization and direction. Shown in comparison the noise curves for the first LIGO interferometer (dashed curve).

2. LIGO-VIRGO INTERFEROMETERS

The other kind of detector for gravitational waves is based on the issue of interferometry known from optics. A laser interferometer gravitational wave detector consists of four masses

that hang from vibration-isolated supports as shown in figure 5, and the indicated optical system for monitoring the separation between the masses. Two masses are near each other, at the corner of an "L", and one mass is at the end of each of the L's long arms. The arm lengths are nearly equal, $L_1 \simeq L_2 = L$. When a gravitational wave, with frequencies high compared to masses, passes through the detector, it pushes the masses back and forth relative to each other as though they were free from their suspension wires, thereby changing the arm-length difference, $\Delta L \equiv L_1 - L_2$. If the waves are coming from overhead or underfoot and the axis of the + polarization coincide with the arm's directions, then it is the + polarization that drives the masses, and $\Delta L(t)/L = h_+(t)$. More generally, the interferometer is sensitive to a linear combination of the two wave fields:

$$\frac{\Delta L(t)}{L} = F_+ h_+(t) + F_\times h_\times(t) \equiv h(t). \tag{37}$$

The coefficients F_+ and $F_\times$ are of the order of unity and depend in a quadrupolar manner on the direction to the source and the orientation of the detector. Usually they are called $beam-pattern functions$. The combination $h(t)$ of the two waveforms is called the $gravitational-wave-strain$ that acts on the detector; and the time evolutions of $h(t)$, $h_+(t)$, and $h_\times(t)$ are sometimes called $waveforms$.

The detector's masses at present are made of transparent fused silica (quartz), though other materials might be used in the future. The masses' inner faces (shown white in the diagram) are covered with high-reflectivity dielectric coatings to form the indicated mirrors, while the masses' outer faces are covered with anti-reflection coatings. The two mirrors facing each other on each arm form a Fabry-Perot cavity. A beam splitter splits a carefully prepared laser beam in two, and directs the resulting beams down the two arms. Each beam penetrates through the antireflection-coating of each arm's corner mass, through the mass, and through the dielectric coating (the mirror); and thereby —if the length of the arm's Fabry-Perot cavity is accurately adjusted —the beam gets trapped in the cavity. The cavity's end mirror has much higher reflectivity than it's corner mirror, so the trapped light leaks back out through the corner mirror, and then hits the beam splitter where it

recombines with light from the other arm. Most of the recombined light goes back toward the laser (where it can be reflected back into the interferometer by a so called light recycling mirror, labeled R), but a tiny portion goes toward the photodiode.

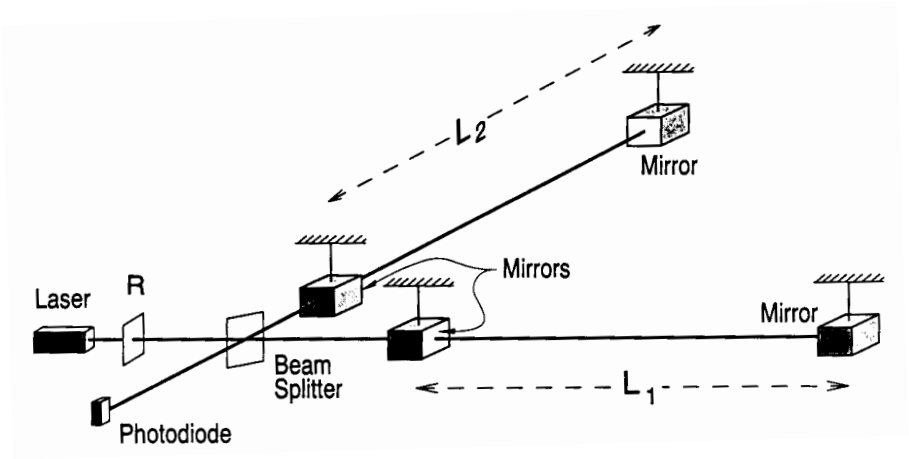

FIG. 5. A simple schematic diagram of a laser interferometer gravitational wave detector

When a gravitational wave hits the detector and moves the masses, thereby changing the lengths L_1 and L_2 of the two cavities, it shifts each cavity's resonant frequency slightly relative to the laser frequency, and thereby changes the phase of the light in the cavity and the phase of the light that exits from the cavity toward the beam splitter. Correspondingly, the relative phase of the two beams returning to the splitter is altered by an amount $\Delta\Phi \propto \Delta L$, and this relative phase shift causes a change in the intensity of the recombined light at the photodiode, $I_{\rm pd} \propto \Delta\Phi \propto \Delta L \propto h(t)$. Thus, the photodiode output current is directly proportional to the gravitational wave strain $h(t)$. This method of monitoring $h(t)$, is capable of very high sensitivity, as we shall see below.

The technology and techniques for such interferometers have been under development for more than 20 years and plans for km-scale interferometers have been developed the past 20 years. Two km-scale systems have recently been approved for construction: the American LIGO ("Laser Interferometer Gravitational-wave Observatory"), and the French/Italian VIRGO (named after the Virgo cluster of galaxies).

LIGO will consist of two vaccum facilities with 4-kilometer-long arms, one in the north-

western part of the USA and the other in the southern-east part of the USA. VIRGO entails one vaccum facility in Pisa, with 3-kilometer-long arms. Both LIGO and VIRGO are scheduled for completion in the late 1990s.

LIGO alone, with it's two sites which have parallel arms, will be able to detect an incoming gravitational wave, measure its two waveforms, and locate its source to within a $\sim 1^\circ$ wide annulus on the sky. LIGO and VIRGO together will be able to locate the source (via time delay, which will be discussed in Sec. IV) to within a 2-dimensional error box with size between several tens of arcminutes and several degrees, depending on the source direction and on the amount of high-frequency structure in the waveforms; and they will be able to monitor both waveforms $h_+(t)$ and $h_\times(t)$.

The accuracies of the direction measurements and the ability to monitor more than one waveform will be severely compromised when the source lies anywhere near the plane formed by the three LIGO/VIRGO interferometer locations. To get good all-sky coverage will require a fourth interferometer at a site far out of that plane; Japan and Australia would be excellent locations, and research groups are carrying out research and development on interferometric detectors, aimed at such a possibility.

Interferometers are plugged by non-Gaussian noise, e.g. due to sudden strain releases in the wires that suspend the masses. This noise prevents a single interferometers, by itself, from detecting with confidence short-duration gravitational-waves bursts. The non-Gaussian noise can be removed by cross correlating two or more interferometers at widely separated sites.

The principal sources of displacement noise are seismic vibrations of the ground beneath the interferometer, and thermally-induced vibrations of the test masses and of the wires that suspend them. Another source of noise in the phase shift is the photon shot noise due to random times at which the light's photons arrive at the photodiode. Figure 6 shows the spectra that are expected from these three noises in the first interferometers that will operate in LIGO. At frequencies above 200 Hz, shot noise dominates; between 200 Hz and 40 Hz, thermal noise in the suspension wires dominates; and below 40 Hz, seismic noise dominates.

During LIGO' s operation, step-by-step improvements will be made in the control of the three noise sources, thereby pushing the overall noise spectrum downward from the "first-interferometer" level toward the "advanced interferometer" level shown in Fig. 6.

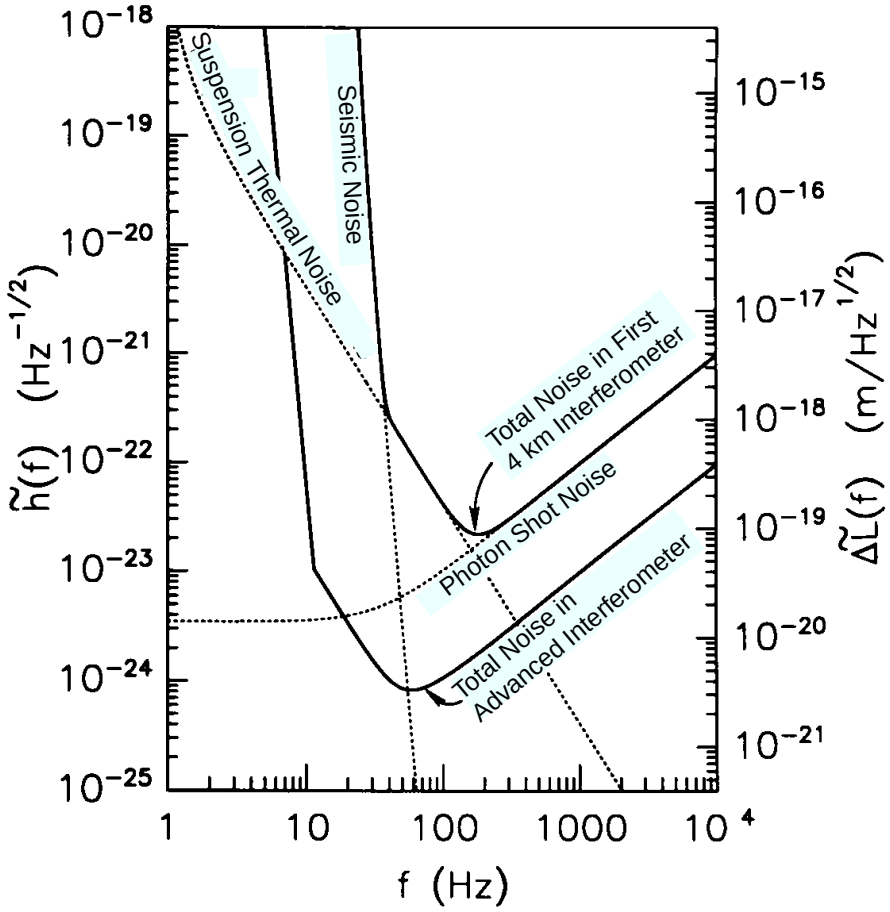

FIG. 6. The expected noise spectrum in each LIGO's first 4-km interferometers (upper solid curve) and in more advanced interferometers (lower solid curve). The dashed curves show various contributions to the first interferometers' noise. Plotted horizontally is gravity wave frequency f; plotted vertically is $\tilde{h}(f)$, the square root of the spectral density of the detectors output $h(t) = \Delta L(t)/L$ in the absence of a gravity wave. The rms noise in a bandwidth Δf at a frequency f is $h_{\rm rms} = \tilde{h}(f)\sqrt{\Delta f}$.

The strongest gravitational waves that arrive at Earth several times per year are expected to have strengths $h \sim 10^{-22}$. Correspondingly, LIGO is designed to achieve rms noise levels $h_{\rm rms} = \tilde{h}(f)\sqrt{\Delta f} \simeq 3 \times 10^{-22}$ in the first detectors, and $\sim 10^{-23}$ in more advanced

detectors. A wave strain $h \simeq 10^{-22}$ will produce a displacement $\Delta L = hL \simeq 10^{-16}$ cm of the interferometer's mirror-endowed masses. 10^{-16} cm is awfully small: 1/1000 the diameter of the nucleus of an atom, and 10^{-12} the wavelength of the light being used to monitor the masses' motion. How can one possibly monitor such small motions?

One adjusts the reflectivities of the interferometer's inner mirrors so that the two arms store laser light on average for about half a cycle of a ~ 100 Hz gravitational wave, which means for about 100 round trips. The light in each arm thereby acquires a phase shift

$$\Delta\Phi \simeq 100 \times \frac{4\pi\Delta L}{\lambda} \simeq 10^{-9}, \tag{38}$$

where $\lambda \simeq 10^{-4}$ cm is the wavelength of light. If the interference of the light from the two beams is done optimally, then this phase shift (equal and opposite in the two arms) can be measured at the photodiode to an accuracy that is governed by the light's photon shot noise, $\Delta\Phi \simeq 1/\sqrt{N}$, where N is the number of photons that enter the interferometer from the laser during the half-cycle of photon storage time. Thus, to achieve the required accuracy, $\Delta\Phi \simeq 10^{-9}$, in the face of photon shot noise, requires $N = 10^{18}$ photons in 0.01 second, which means a laser power of ~ 100 Watts.

By cleverness, one can reduce the required laser power: The light is stored in the interferometer arms for only a half gravity-wave period (~ 100 round tips) because during the next half period the waves would reverse the sign of ΔL, thereby reversing the sign of the phase shift being put onto the light and removing from the light the signal that had accumulated in the first half period. In just 100 round tips, however, the light is attenuated hardly at all. One therefore reuses the light over and over again. This is done by (i) operating the interferometer with only a tiny fraction of the recombining light going out toward the photodiode, and almost all of it instead is going back toward the laser, and by (ii) placing a mirror between the laser and the interferometer in just such a position that the entire interferometer with each arms as two subcavities become an optical cavity driven by the laser. Then mirror R recycles the recombining light back into the interferometer in phase with the new laser light, thereby enabling a laser of say 5 Watts to perform like one

of 100 Watts or more.

Turn from photon shot noise to thermal noise. How, one might ask, can somebody possibly expect to monitor the mirror's motions at a level of 10^{-16} cm when the room temperature atoms of which the fused-silica mirrors are made vibrate thermally with amplitudes $\Delta l_{\rm rms} = \sqrt{kT/m\omega^2} \simeq 10^{-10}$ cm? The answer is that these individual atomic vibrations are unimportant. The light beam, with its $\sim$ 5 cm diameter, averages over the positions of $\sim 10^{21}$ atoms in the mirror, and with its 0.01 sec storage time it averages over $\sim 10^{11}$ vibrations of each atom. This spatial and temporal averaging makes the vibration of the individual atoms irrelevant. Not so irrelevant, however, are the lowest-frequency normal-mode vibrations of the mirror-endowed masses (since this mode experience much less time averaging than the fast atomic vibrations). Assuming a mass m $\sim$ (a few tens of kg), these normal modes have angular frequencies $\omega \simeq 10^5 s^{-1}$, so their rms vibration amplitude is $\Delta l_{\rm rms} = \sqrt{kT/m\omega^2} \simeq 10^{-14}$ cm. This is 100 times larger than the signals we wish to monitor; but if this modes have high quality factor, then the vibrations will be very steady over the interferometer's averaging time of 0.01 sec; and correspondingly these effects will average down by more than a factor 100. Similar considerations apply to the thermal noise in the masses suspention wires.

Finally turn from thermal noise to seismic noise. At the LIGO sites, and most any other quiet location on Earth, the ground is continually shaking with an rms displacement $\Delta l_{\rm rms} \simeq 10^{-8} cm (100 Hz/f)^{3/2}$. This is 10^7 times larger than the the motions one seek to monitor. At frequencies above 10 Hz or so, one can protect the masses from these seismic vibrations by simple passive isolation stacks. Each element in the stack is a mass and a spring with normal-mode frequency $f_0 \sim$ (a few Hz). When seismic noise tries to drive this harmonic oscillator far above its resonant frequency, the amplitude of its response is attenuated relative to the driving motion by a factor $(f_0/f)^2$. Thus, each oscillator in the stack will provide reduction 10^2 in $\Delta l_{\rm rms}$, so a stack of four or five oscillators are enough to provide the required isolation.

The above rough estimates show that it is possible for interferometers to achieve the

required sensitivities, $h_{\rm rms} \simeq 10^{-22}$ and $\Delta L \simeq 10^{-16}$ cm. However, going out from these rough estimates to a real working interferometer, and doing so in the face of a plethora of other noise sources, is a tremendous experimental challenge that has occupied a number of excellent experimental physicists since 1972.

3. LISA : The Laser Interferometric Space Antenna

LISA the Laser Interferometric Space Antenna is planned to operate the second decade of the 21=st century. The main economic source of the program is ESA (European Space Agency) but members of the LISA team hope that NASA will join together with ESA so that the project will be completed considerably sooner.

LISA will consist of six compact drag-free spacecraft (i.e spacecraft that are shielded from buffeting by solar wind and radiation pressure, and that thus move very nearly at a geodesics of spacetime). All six spacecraft will be launched simultaneously by a single Ariane rocket. They would be placed into the same heliocentric orbit as the Earth occupie, but would follow 20° behind the Earth as shown in figure 7. The spacecraft would fly in pairs, with each pair at a vertex of an equilateral triangle that is inclined at an angle of 60° to the Earth's orbital plane. The triangle's arm length would be 5 million km (10^6 larger that LIGO's arms). The six spacecraft would track each other optically, using one—Watt Laser beams. Because of diffraction losses over the 5×10^6 km arm length, it is not feasible to reflect the laser beams back and forth as is done in LIGO. Instead, each spacecraft will have it's own laser; and the lasers will be phase locked to each other, thereby achieving the same kind of phase—coherent out and back light as LIGO achieves with mirrors. The six laser, six spacecraft configuration thereby functions as three, partially independent by partially redundant gravitational-wave interferometer.

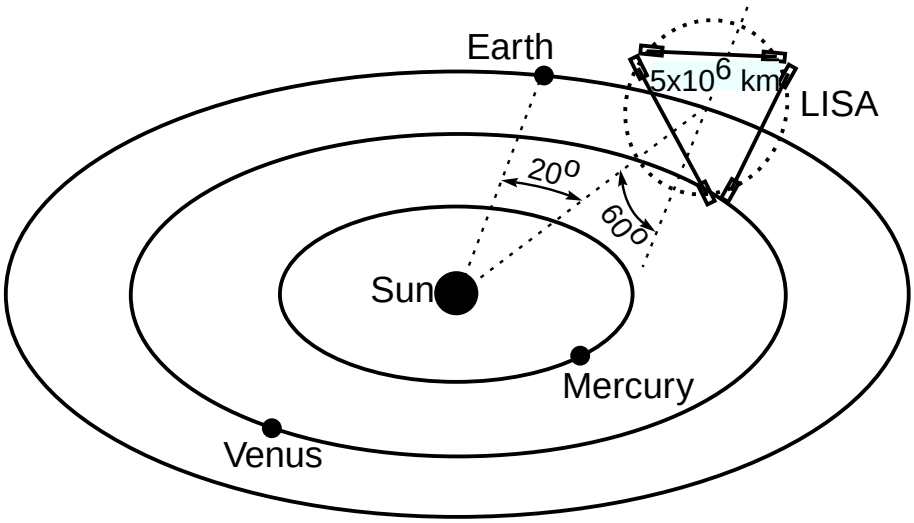

FIG. 7. LISA's orbital configuration

Figure 8 shows the expected noise and sensitivity of LISA in the same language as we have used for LIGO (Fig 6). The curve at the bottom of the stippled region is $h_{\boldsymbol{r}_{ms}}$, the rms noise, in a bandwidth equal to frequency, for waves with optimum direction and polarization. The top of the stippled region is $h_{\boldsymbol{S}_B} = 5\sqrt{5}h_{\boldsymbol{r}_{ms}}$, the sensitivity for high-confidence detection ($S/N = 5$) of a broad-band burst coming from random direction, assuming Gaussian noise.